University of Huddersfield Repository

Forsyth, David I., Wade, Scott A., Sun, Tong, Chen, Xiaomei and Grattan, Kenneth T. V.

Dual Temperature and Strain Measurement with the Combined Fluorescence Lifetime and Bragg Wavelength Shift Approach in Doped Optical Fiber

Original Citation

Forsyth, David I., Wade, Scott A., Sun, Tong, Chen, Xiaomei and Grattan, Kenneth T. V. (2002) Dual Temperature and Strain Measurement with the Combined Fluorescence Lifetime and Bragg Wavelength Shift Approach in Doped Optical Fiber. Applied Optics, 41 (31). p. 6585. ISSN 0003-6935

This version is available at http://eprints.hud.ac.uk/id/eprint/15602/

http://eprints.hud.ac.uk/

Dual temperature and strain measurement with the combined fluorescence lifetime and Bragg wavelength shift approach in doped optical fiber

David I. Forsyth, Scott A. Wade, Tong Sun, Xiaomei Chen, and Kenneth T. V. Grattan

We have constructed fiber-optic sensors to measure temperature and strain by combining the properties of fiber Bragg gratings with the fluorescent lifetimes of various doped fibers. Sensors have been made with the fiber Bragg grating written directly into the doped fiber to ensure the collocation of the strain and temperature measurement points. Results are compared with those obtained previously from a Bragg grating written into standard photosensitive fiber spliced to doped fiber. Standard deviation errors of 7 $\mu\epsilon$ and 0.8 °C have been obtained for strain and temperature ranges of up to 1860 $\mu\epsilon$ and 120 °C, respectively. © 2002 Optical Society of America

OCIS codes: 060.2370, 160.5690.

1. Introduction

The simultaneous measurement of both temperature T and strain ϵ is highly desirable in a range of industrial applications, e.g., structural monitoring with embedded sensors where a temperature-compensated strain measurement is important, and many varied and interesting schemes have been reported over a number of years to produce fiber optical sensors to facilitate such measurements.[1,2] Some of the sensors developed in this way are relatively simple in construction but many involve complex optical decoding of the signals produced. The most direct way to measure these parameters in this type of situation is to use physically separate sensors, where one is isolated from the strain to provide temperature measurement and thus the compensation inevitably needed for the sensor experiencing both temperature and strain changes. However, where sensors need to be embedded within a certain structure so as to be fully integrated, then the idea of a second sensor becomes almost impractical if it is collocated and simultaneous measurement is needed. So in most cases a robust, compact sensor is required, allowing simple sensor discrimination and thus a situation in which the measurands of interest can be easily determined.

Methods based on fiber Bragg gratings (FBGs) alone[3] often require two separate gratings to allow for temperature compensation purposes. It is well known[4] that a single grating used as a stand-alone temperature or strain sensor will show unwanted cross sensitivity to either parameter (at levels typically of 10 pm/°C and 1 pm/$\mu\epsilon$, respectively), and errors that have been reported are generally in the region of 1 °C and 10–25 $\mu\epsilon$ for such schemes. Bragg grating-based devices have a demonstrated capability for use in multiplexed sensor arrangements to create effective quasi-distributed systems. In the area of fully distributed sensing, considerable progress has been made with intrinsic scattering techniques (e.g., Brillouin scattering[5]), but at the expense of having to use sophisticated and costly optoelectronic techniques. In some of the many other techniques reported, Jung and co-workers[6,7] have demonstrated simultaneous strain and temperature measurement using the amplified spontaneous emission power of Er^{3+} and Er^{3+}:Yb^{3+}-doped fiber combined with a FBG, but the relatively long length of doped fiber required to achieve the desired level of signal amplification (7 m for Er^{3+} and 25 cm for Er^{3+}:Yb^{3+}) and the dependence of the amplified spontaneous emission power on the excitation power are

D. I. Forsyth, S. A. Wade, T. Sun, and K. T. V. Grattan (k.t.v.grattan@city.ac.uk) are with the School of Engineering, City University, Northampton Square, London EC1V 0HB, United Kingdom. S. A. Wade is also with the Optical Technology Research Laboratory, Victoria University, P.O. Box 14428 Melbourne City MC, Victoria 8001, Australia. X. Chen is with the Changcheng Institute of Metrology, P.O. Box 1066, Beijing 100095, China.

limitations. Lai and co-workers have managed to overcome these sensor size and pump-power-dependency problems in their currently developing research based on a similar technique,[8] which parallels the approach taken in our study here.

Fluorescence-based sensing is well known as the basis of several intrinsic fiber sensor devices for the measurement of temperature,[9,10] and the rare-earth-doped fiber commonly used is available at relatively low cost. Excitation of fluorescence from many of these fibers can be achieved with a range of widely available sources, and the detection of the fluorescence is usually a straightforward process. In addition, the in-fiber nature of the sensors makes them readily compatible with a range of other fiber-optic sensor schemes. A number of recent research papers have shown that, in addition to the well-known temperature dependence, the fluorescence lifetime and intensity ratio techniques also show an additional but much smaller strain dependence,[11–16] which in many situations can be ignored.

From this research, the strain sensitivity of the lifetime has been shown to be generally in the region of 10^{-2} to 10^{-4} μs/$\mu\epsilon$ for silica rare-earth-doped fibers, but the origin of this strain sensitivity of fluorescence lifetime is still the subject of some discussion.[17] It is possible that this may be due to shifts in the energy levels as a function of strain, as has been reported previously in crystals for high-pressure tests.[18] Further research to investigate this effect is currently under way. On the other hand, a physical origin of the strain sensitivity of the fluorescence from rare-earth-doped fiber has also been suggested in recent research[19] to be due to a temporary volumetric distortion of the energy-transfer rates between the dopant ions, caused by a slight decrease in the dopant concentration within a fiber when subjected to strain. Modeling of the latter[20] has been shown to account well for the fluorescent lifetime temperature and strain dependence with Nd^{3+}-doped fibers, and this likely can be extrapolated for other doped rare-earth dopants.

Therefore, rather than use the change in the fluorescence parameters to determine strain (complicated by being convoluted with the temperature change), we decided to investigate two potentially simpler and more compact optical fiber sensor configurations. These comprise two unique sensor schemes in which a combination of a FBG and the fluorescence decay within short lengths (a few centimeters) of doped fiber are used. These schemes take advantage of the intrinsic properties of FBGs as well as exploiting the fluorescence properties (i.e., lifetime change with temperature and strain) of short lengths of doped fiber, which have previously yielded satisfactory results in research performed recently by some of the authors in a similar sensor scheme using a separate FBG component spliced to a short length of Er^{3+}-doped fiber for the first time to our knowledge for such dual measurement.[21] Here, those results obtained previously (under similar experimental conditions) are compared with results from the new sensor

configurations in which the FBGs are directly written into the doped fibers, thus eliminating the need for two separate components in one sensor system and enabling a collocation of the sensor elements.

The theory behind this research has been discussed in some detail by Jones.[1] In the case in which two measurand-dependent observables τ (fluorescent lifetime) and λ (FBG wavelength) are obtained at a certain temperature T and a specific strain ϵ, this can be represented by the following matrix equation:

$$\begin{bmatrix} \Delta\tau \\ \Delta\lambda \end{bmatrix} = \begin{bmatrix} K_{1T} & K_{1\epsilon} \\ K_{2T} & K_{2\epsilon} \end{bmatrix} \begin{bmatrix} T \\ \epsilon \end{bmatrix}, \qquad (1)$$

such that

$$\begin{bmatrix} T \\ \epsilon \end{bmatrix} = \frac{1}{K_{1T}K_{2\epsilon} - K_{2T}K_{1\epsilon}} \begin{bmatrix} K_{2\epsilon} & -K_{1\epsilon} \\ -K_{2T} & K_{1T} \end{bmatrix} \begin{bmatrix} \Delta\tau \\ \Delta\lambda \end{bmatrix}, \qquad (2)$$

where K_{nT} and $K_{n\epsilon}$ are the temperature and strain coefficients corresponding to the change in the fluorescence lifetime $\Delta\tau(n = 1)$ and the change of the FBG wavelength $\Delta\lambda(n = 2)$.

2. Experimental Arrangement

A previously reported sensor with a FBG and fluorescent fiber combination has been[19] discussed by some of the authors and is labeled here as sensor 1. It utilized an individual FBG (written in plain photosensitive fiber, 1548-nm center wavelength) spliced to a small length (5 cm) of single-mode 4370-parts per million (ppm wt.) Er^{3+}-doped fiber. Two different sensing elements were developed for the next stage of this particular study. The first sensor was made with the FBG at a center wavelength of 1551.5 nm, which was chosen because of the ready availability of a phase mask and the Er^{3+}-doped fiber that fluoresces in this spectral region. This is, of course, the wavelength favored for optical communications purposes. The FBG was written into a 16-cm length of (5–125-μm core–cladding diameter) 1050-ppm Er^{3+}-doped fiber (termed sensor 2) by a KrF excimer laser centered at 248 nm, before which the Er^{3+}-doped fiber was hydrogen loaded for one week to enhance its photosensitivity. The second sensor was designed with the FBG (1549.7-nm center wavelength) written into a 12-cm length of single-mode Er^{3+}:Yb^{3+} co-doped fiber (termed sensor 3). For sensor 3, the co-doped fiber was of unique construction in that it had been designed with a photosensitive ring (during the manufacturing process), and the grating was written with a frequency-doubled argon-ion laser (244 nm), thus not requiring prior hydrogen loading of the fiber. This fiber had a cladding diameter of 125 μm; a numerical aperture of 0.2; and core dopants of Er^{3+}, Yb^{3+}, and aluminum. Results from both of these schemes are compared with those obtained from sensor 1.

During the sensor calibration tests, the sensing elements were centered within the temperature-controlled zone of a stabilized oven (Carbolite), as shown schematically in Fig. 1. In addition to tem-
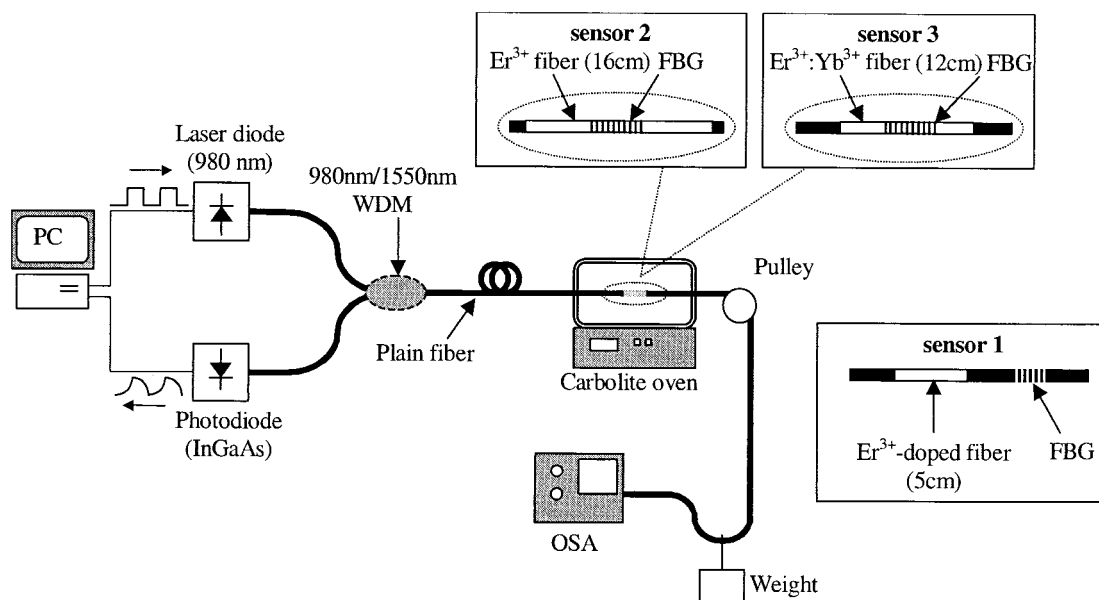
Fig. 1. Experimental arrangement used for the temperature and strain calibration of the sensors (sensors 1, 2, and 3 shown as insets). OSA, optical spectrum analyzer.

perature control, the experimental arrangement allowed a range of strains to be applied to the sensor at various temperatures (those from ambient to a maximum of 150 °C were used during these calibration tests to avoid thermal damage to the FBG). A 980-nm laser diode, with an output power of approximately 2 mW, was employed to pump the doped fiber under test, and its output was modulated by a computer-generated trigger pulse. We achieved excitation of the doped fiber by coupling the output of the laser diode to the 980-nm input port of a 2×1 980–1550-nm wavelength division multiplexing (WDM) coupler arrangement, and fluorescence in the 1550-nm region was detected with the output port. As in previous research, a pulley system was used to apply strain to the dual fiber sensor, where the mass m that was added determined the overall strain exerted on the test fiber. This strain applied to the sensing fiber ϵ was calculated by the relationship

$$\epsilon = \frac{m.g/A}{Y}, \qquad (3)$$

where A is the cross-sectional area of the fiber, g is the acceleration that is due to gravity (9.81 m/s^2), and Y is Young's modulus (7.31×10^{10} N/m^2 for fused quartz). Care was taken to prevent the fiber from touching the glass lining of the tube oven and to lubricate the pulley to minimize friction for better repeatability of the test measurements. We employed an InGaAs photodiode to measure the fluorescence emission at the 1550-nm wavelength from both the Er^{3+} and the $Er^{3+}:Yb^{3+}$ codoped fiber sensors (in the latter case enhanced by the direct energy transfer from the Yb^{3+} to the Er^{3+} ions present[22]) by connecting it to the other input port of the WDM coupler. In this paper, for simplicity, the measurement of the

FBG wavelength shift was achieved with a commercial (Agilent) optical spectrum analyzer with a resolution bandwidth of 0.1 nm. It should be noted that several relatively inexpensive dedicated systems for measurement of these FBG wavelength changes have been discussed in the literature.[23,24]

The fluorescence lifetime of the doped fibers was measured with an analog-to-digital card connected to a computer, which sampled the output of the photodiode, this being triggered by the falling edge of the excitation pulse. The value of the fluorescence lifetime was subsequently obtained by Prony's method, as discussed in a previous paper.[25] We made the measurements of the center wavelength of the FBG by recording and analyzing the transmission dip in the fluorescence spectra of the doped fibers. This emphasizes a particularly attractive aspect of this approach in that these spectra contain an associated and easily observable feature corresponding to the FBG (as shown in Fig. 2), and thus a second source at a wavelength around 1550 nm is not required. Hence the fluorescence itself that is generated acts as the interrogation light for the FBG, removing the need for additional components. Thus, when we choose, as was done in this case, the wavelength of the FBG to lie within the fluorescence band of the doped fiber, the system incorporated its own fluorescence fiber source. This wavelength measurement with the FBG does not interfere with the measurement of the change in the fluorescence lifetime, which provides the temperature correction.

3. Results and Discussion

A series of calibration tests was performed to assess the performance of the two dual temperature–strain sensor systems (sensor 2 and sensor 3) and to compare the results with previously obtained results
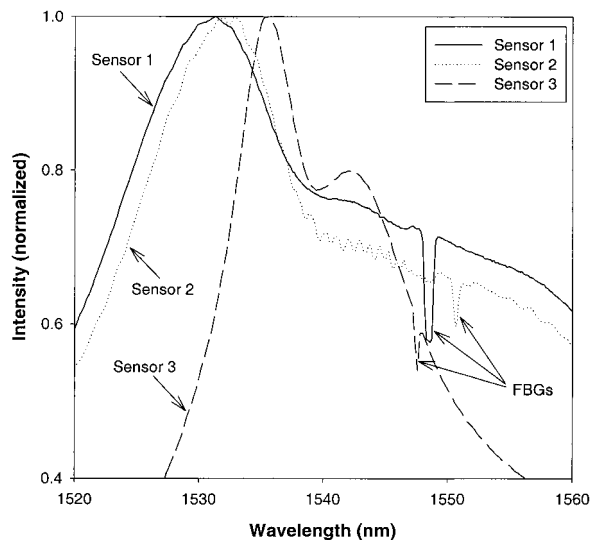
Fig. 2. Fluorescence spectra from all three sensors showing intensity dips that are due to the FBG reflection.

Fig. 4. Shifts in the FBG wavelength with strain for sensor 3 for a range of temperatures tested.

from sensor 1. Measurements of the fluorescence lifetime and the FBG wavelength for both sensors were taken for a range of applied strains from 221 to 1328 $\mu\epsilon$ at temperatures between 30 °C and 150 °C. Measurements of the center wavelength of the FBGs as a function of both temperature and strain resulted
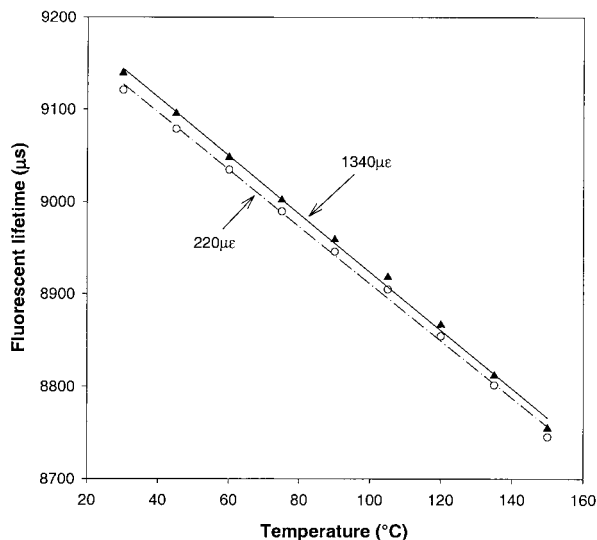

Fig. 3. Fluorescent lifetime versus temperature calibration data for sensor 3 at minimum and maximum applied strains together with linear fits to the data.
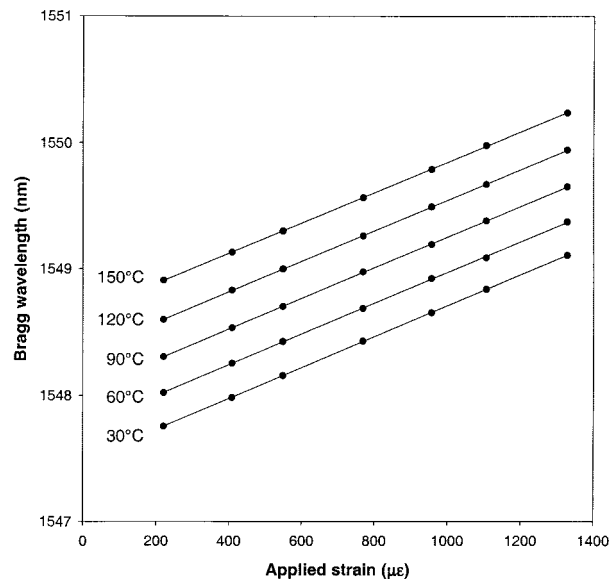
in linear wavelength shifts over the ranges measured for both of the sensor configurations, as expected. Figure 3 shows an example of the change in the fluorescence lifetime with temperature at two different applied strains obtained with sensor 3. An example of the shift in the FBG wavelength as a function of applied strain is given in Fig. 4 for results obtained with sensor 3 at a range of temperatures. The values of the temperature and strain coefficients of the fluorescence lifetime and the FBG wavelength, obtained when straight lines are fit to the data, are given in Table 1. The strain sensitivities (in units of $\mu s/\mu\epsilon$) of all the doped fibers, obtained from straight-line fits to graphs of fluorescence lifetime versus strain at each of the temperatures tested, are plotted as a function of temperature in Fig. 5. The results indicate that the strain sensitivities of the three fibers are essentially similar. It is interesting to note, however, that the strain sensitivity of the Er^{3+}:Yb^{3+} device (sensor 3), as a function of temperature, appears to be less constant than was seen for the others. The reason this may occur could be due to the presence of one of the dopants (in addition to the added Yb^{3+}) that is used in the manufacture of this fiber to achieve a specific refractive index. The presence of these materials may then have some effect on the strain sensitivity, but this will require further study.

Using the coefficients determined above with Eq.

Table 1. Temperature and Strain Coefficients of the Fluorescence Lifetime and the FBG Wavelength for all Three Sensors

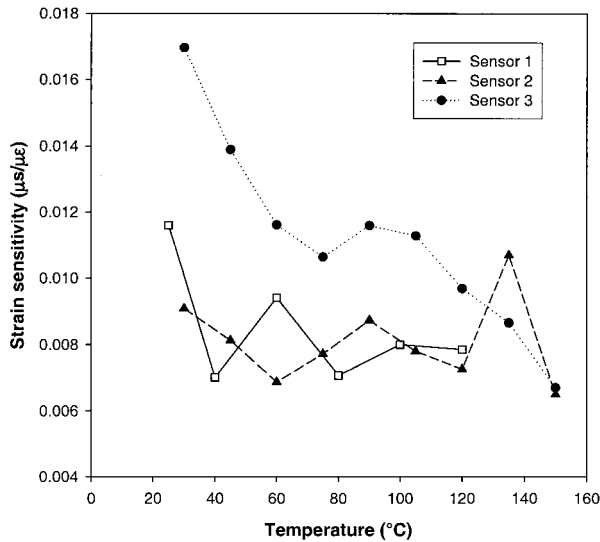| Parameter	Sensor 1	Sensor 2	Sensor 3
K_{1T} ($\mu s/°C$)	-1.65 ± 0.04	-1.76 ± 0.01	-3.11 ± 0.06
$K_{1\epsilon}$ ($\mu s/\mu\epsilon$)	$(8.49 \pm 1.75) \times 10^{-3}$	$(8.08 \pm 1.28) \times 10^{-3}$	$(1.12 \pm 0.01) \times 10^{-2}$
K_{2T} ($nm/°C$)	$(1.03 \pm 0.03) \times 10^{-2}$	$(1.09 \pm 0.01) \times 10^{-2}$	$(0.96 \pm 0.01) \times 10^{-2}$
$K_{2\epsilon}$ ($nm/\mu\epsilon$)	$(1.15 \pm 0.01) \times 10^{-3}$	$(1.22 \pm 0.01) \times 10^{-3}$	$(1.21 \pm 0.01) \times 10^{-3}$

Fig. 5. Comparison of the strain sensitivities of fluorescent lifetimes over the full temperature ranges for all three sensors.
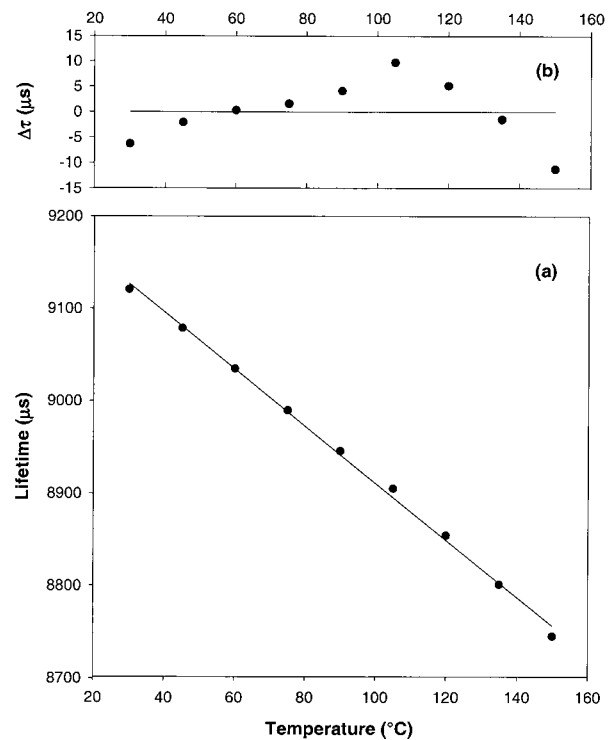

Fig. 6. (a) Fluorescent lifetime versus temperature data obtained at minimum applied strain (221 $\mu\epsilon$). (b) Difference between the experimental data and the linear fit for sensor 3.

(2), we calculated the values of temperature and strain for the data obtained from the optical sensors, and then these were compared with the known conditions applied during these tests. The standard deviation of the differences between the values calculated from the optical data and those applied in the full range of tests for all the sensors studied are recorded in Table 2 and are discussed below.

One of the potential sources of error lies in the assumption in Eqs. (1) and (2) that the measured parameters (i.e., lifetime and FBG wavelength) will have a linear dependency on the measurands (temperature and strain in this case). Previous research[26] has shown this to be a valid assumption for FBGs over the ranges measured here, but research on the fluorescence lifetime, however, suggests a nonlinear temperature dependence when wide temperature ranges are of interest. Figures 6(a) and 6(b) show an example of a linear fit to the temperature dependence of the fluorescence lifetime of sensor 3 (obtained at minimum applied strain) and the difference between the fit and the actual data, indicating a slight nonlinearity. To obtain a more detailed understanding of the effect of this on the errors in the data shown in Table 2, an analysis of the linearity of the fluorescence lifetime versus temperature data was undertaken for the temperature ranges investi-

gated. The r^2 values (the coefficient of determination) obtained for linear fits to the data are listed in Table 3. These values provide a measure of the deviation of the experimental data from linearity, where a value closer to unity indicates better agreement with a linear fit. It can be seen from Table 3 that a value of 0.9996 (for sensor 3) corresponds to the best degree of linearity achieved for temperature measurement by use of the lifetime alone; this also gives the lowest temperature error value of 0.8 °C in Table 2. The value of 0.9973 (for sensor 2) corresponding to an error value of 1.5 °C is the least good in terms of linearity, although satisfactory for a number of measurement situations. Another factor affecting the temperature measurement accuracy is the temperature sensitivity of the fluorescence lifetime, and the errors inherent in the measurement by use of an erbium-doped fiber system have been discussed by some of the authors previously in some detail[27] and are not reproduced here. It is expected that the high temperature sensitivity of the fiber used for sensor 3

Table 2. Standard Deviation of Differences between Temperature and Strain Values Calculated with Measurements from the Optical Sensors and the Known Parameters Applied During the Tests

Sensor	Temperature Range	ΔT (°C)	$\Delta\epsilon$ ($\mu\epsilon$)
1	25–120 °C	1.2	20.4
2	30–120 °C	1.5	21.1
	30–150 °C	1.8	25.7
3	30–120 °C	0.8	7.0
	30–150 °C	1.9	10.7

Table 3. Average r^2 Values Obtained for Linear Fits to Lifetimes Versus Temperature Data for all Three Sensors, Indicating the Linearity of the Fits

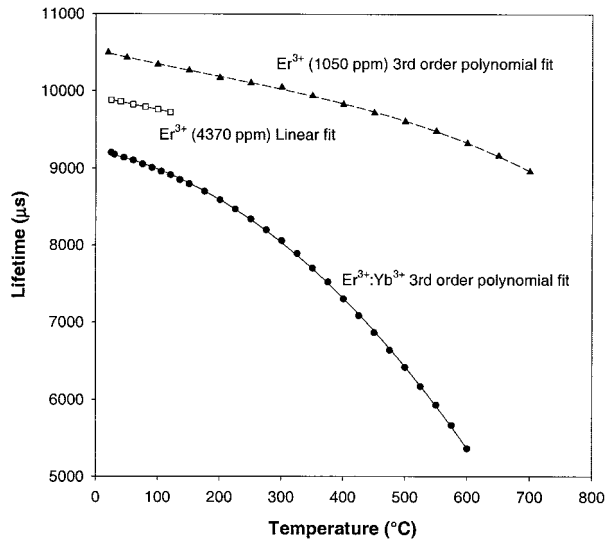| Temperature	Sensor 1	Sensor 2	Sensor 3
25–120 °C	0.9991	—	—
30–120 °C	—	0.9973	0.9996
30–150 °C	—	0.9976	0.9977

Fig. 7. Temperature characteristics of the fluorescent lifetime of all sensors for an extended temperature range.

$(Er^{3+}:Yb^{3+})$ (which, as can be seen from Table 1, is almost twice that of the other two sensors) can enhance its potential performance in practical sensor systems.

Figure 7 shows how the fluorescent lifetime dependence on temperature can be exploited, for dual temperature–strain sensor purposes, within the linear region over the lower temperature ranges. The lifetime and temperature dependence of the Er^{3+} 1050-ppm fiber material used for sensor 2 is much more linear (but the response is less sensitive) over a larger temperature range than for the $Er^{3+}:Yb^{3+}$ codoped fiber material used for sensor 3. Figure 7 displays how the performance of the sensor can be

customized to meet the demands for high temperature sensitivity, measurement range, and good reproducibility.

As mentioned above, the dual sensors tested here make use of temperature–strain discrimination techniques. Figures 8(a) and 8(b) show the importance of the compensation approach when we consider temperature and strain measurements from the Er^{3+}: Yb^{3+} codoped fiber dual sensor (sensor 3) both with and without the compensation provided by the fluorescence lifetime measurements. Figures 8(a) and 8(b) illustrate the significance of when the corrections are applied to the FBG wavelength shift readings that were obtained for a constant temperature [30 °C in this case for Fig. 8(a)] and a constant strain measurement of 220 $\mu\epsilon$, respectively [for Fig. 8(b)]. It is obvious from the graphs that, without compensation provided by the lifetime measurement, these types of sensor would show a serious measurement error, e.g., adding a strain of 1000 $\mu\epsilon$ would cause the temperature to be read as approximately 125 °C instead of the actual 30 °C [as shown in Fig. 8(a)] and similarly at 125 °C a strain value of approximately 1000 $\mu\epsilon$ would be recorded instead of the real applied value of 220 $\mu\epsilon$ [as shown in Fig. 8(b)].

4. Conclusion

We have reported the results of unique and simple sensor schemes, capable of effective temperature–strain discrimination with single sensing elements, which show considerable potential for further development. These sensors utilize the current versatility and effectiveness of Bragg gratings (e.g., ease of WDM, an effective linear temperature–strain response, interruption of immunity, and ability for multiplexing) and exploit the temperature–strain
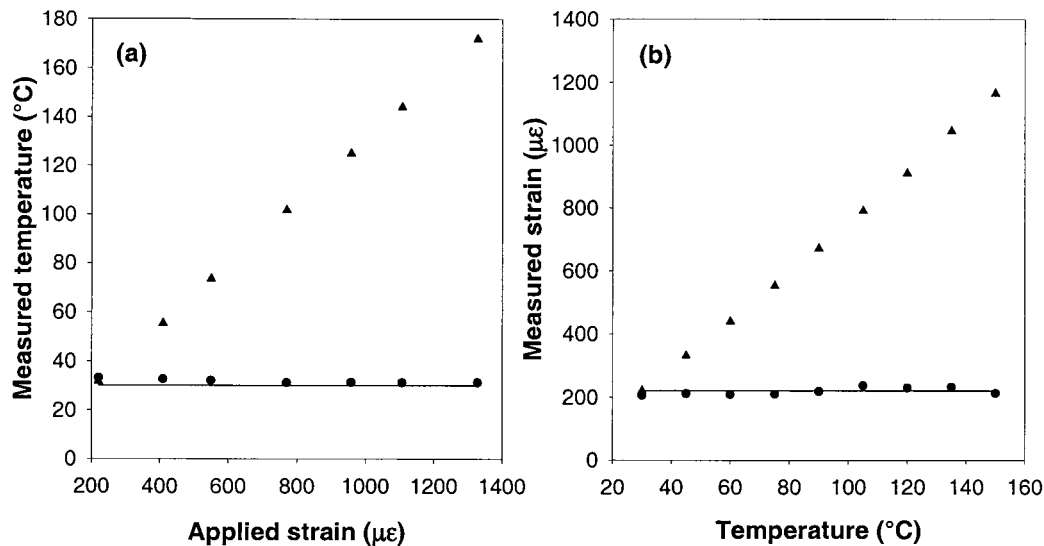

Fig. 8. (a) Fluorescent lifetime correction of Bragg shifts at constant temperature (30 °C) and (b) at constant strain (221 $\mu\epsilon$) for sensor 3. The values obtained from FBG data alone are displayed as filled triangles, and the values obtained with the combined FBG and fluorescence lifetime approach are shown as filled circles. The straight lines show the constant temperature (30 °C) and strain (221-$\mu\epsilon$) values to which the sensor was exposed.

dependency of the fluorescence lifetime from doped fiber. In addition, use of the fluorescence generated within the optical system to interrogate the FBG provides a major advantage in that no external light source is required. The sensor elements are conveniently collocated on one fiber, for ease of installation and use, and the size of the active region is small, facilitating both point sensor use and offering the potential for multiplexing of the sensors along a single fiber for distributed measurement. Applications such as in large-scale civil engineering monitoring (e.g., the structural integrity of a bridge) are therefore possible. Research is continuing to determine which materials are best to use for optimization in a range of different practical compromises, e.g., smart structures where sensors need to be embedded and coated for such use, and also to achieve an improvement in the resolution of both parameters. In addition, the issues of long-term stability and wider utility are being considered.

References

1. J. D. C. Jones, "Review of fibre sensor techniques for temperature-strain discrimination," in *Optical Fiber Sensors*, Vol. 16 of OSA Technical Digest Series (Optical Society of America, Washington, D.C., 1997), pp. 36–39.

2. W. Jin, W. C. Michie, G. Thursby, M. Konstantaki, and B. Culshaw, "Simultaneous measurement of strain and temperature: error analysis," Opt. Eng. **36,** 598–609 (1997).

3. Y. J. Rao, N. Fisher, P. Henderson, V. Lecouche, C. N. Pannell, D. J. Webb, and D. A. Jackson, "Recent developments in fibre optic sensors for point and distributed sensing in large structures," in *European Workshop on Optical Fibre Sensors*, B. Culshaw and J. D. C. Jones, eds., Proc. SPIE **3483,** 138–141 (1998).

4. Y. J. Rao, "Review article: in-fibre Bragg grating sensors," Meas. Sci. Technol. **8,** 355–375 (1997).

5. T. R. Parker, M. Farhadiroushan, V. A. Handerek, and A. J. Rogers, "A fully distributed simultaneous strain and temperature sensor using spontaneous Brillouin backscatter," IEEE Photon. Technol. Lett. **9,** 979–981 (1997).

6. J. Jung, H. Nam, J. H. Lee, N. Park, and B. Lee, "Simultaneous measurement of strain and temperature by use of a single-fiber Bragg grating and an erbium-doped fiber amplifier," Appl. Opt. **38,** 2749–2751 (1999).

7. J. Jung, N. Park, and B. Lee, "Simultaneous measurement of strain and temperature by use of a single fiber Bragg grating written in an erbium:ytterbium-doped fiber," Appl. Opt. **39,** 1118–1120 (2000).

8. Y. C. Lai, G. F. Qiu, W. Zhang, L. Zhang, I. Bennion, and K. T. V. Grattan, "Simultaneous measurement of temperature and strain by combining active fibre with fibre gratings," in *Proceedings of Sensors and their Applications XI*, K. T. V. Grattan and S. H. Khan, eds. (Institute of Physics, London, 2001), pp. 135–139.

9. K. T. V. Grattan and Z. Y. Zhang, *Fiber Optic Fluorescent Thermometry* (Chapman & Hall, London, 1995).

10. S. F. Collins, G. W. Baxter, S. A. Wade, T. Sun, K. T. V. Grattan, Z. Y. Zhang, and A. W. Palmer, "Comparison of fluorescence-based temperature sensor schemes: theoretical analysis and experimental validation," J. Appl. Phys. **84,** 4649–4654 (1998).

11. T. Liu, G. F. Fernando, Z. Y. Zhang, and K. T. V. Grattan, "Simultaneous strain and temperature measurements in composites using extrinsic Fabry-Perot interferometric and intrinsic rare-earth doped fibre sensors," in *Sensory Phenomena and Measurement Instrumentation for Smart Structures and Materials*, R. O. Claus and W. B. Spillman, eds., Proc. SPIE **3330,** 332–341 (1998).

12. T. Sun, Z. Y. Zhang, K. T. V. Grattan, and A. W. Palmer, "Intrinsic doped fluorescence decay-time based measurements: strain and temperature characteristics for sensor purposes," Rev. Sci. Instrum. **69,** 4186–4190 (1998).

13. T. Sun, Z. Y. Zhang, K. T. V. Grattan, and A. W. Palmer, "Intrinsic strain and temperature characteristics of Yb-doped silica-based optical fibers," Rev. Sci. Instrum. **70,** 1447–1451 (1999).

14. A. Arnaud, D. I. Forsyth, T. Sun, Z. Y. Zhang, and K. T. V. Grattan, "Strain and temperature effects on erbium-doped fiber for decay-time based sensing," Rev. Sci. Instrum. **71,** 104–108 (2000).

15. J. H. Sharp and H. C. Seat, "Temperature and strain characteristics of ruby fibre fluorescence emission," in *14th International Conference on Optical Fiber Sensors*, A. G. Mignani and H. C. Lefèvre, eds., Proc. SPIE **4185,** 54–57 (2000).

16. S. A. Wade, S. F. Collins, G. W. Baxter, and G. Monnom, "Effect of strain on temperature measurements using the fluorescence intensity ratio technique (with Nd^{3+}- and Yb^{3+}-doped silica fibers)," Rev. Sci. Instrum. **72,** 3180–3185 (2001).

17. D. I. Forsyth, S. A. Wade, D. Perciante, and K. T. V. Grattan, "Temperature and strain characteristics of the $^3F_4$ and $^3H_4$ energy levels of Tm:Ho co-doped fibre," in *Proceedings of Sensors and their Applications XI*, K. T. V. Grattan and S. H. Khan, eds. (Institute of Physics, London, 2001), pp. 365–370.

18. Th. Tröster, T. Gregorian, and W. B. Holzapfel, "Energy levels of Nd^{3+} and Pr^{3+} in RCL_3 under pressure," Phys. Rev. B **48,** 2960–2967 (1993).

19. P. M. Farrell, S. A. Wade, G. W. Baxter, S. F. Collins, A. J. Stevenson, and K. T. V. Grattan, "On the physical origin of strain sensitivity in optical fibre rare earth fluorescence sensors," in *Proceedings of Sensors and their Applications XI*, K. T. V. Grattan and S. H. Khan, eds. (Institute of Physics, London, 2001), pp. 231–236.

20. S. F. Collins, P. M. Farrell, S. A. Wade, G. W. Baxter, D. A. Simpson, A. J. Stevenson, K. T. V. Grattan, and D. I. Forsyth, "Modelling strain dependence of fluorescence from doped optical fibres: application to neodymium," presented at Conference of Optical Fiber Sensors 2002, Portland, Ore., 6–10 May 2002.

21. S. A. Wade, D. I. Forsyth, Q. Guofu, and K. T. V. Grattan, "Fiber optic sensor for dual measurement of temperature and strain using a combined fluorescent lifetime decay and fiber Bragg grating technique," Rev. Sci. Instrum. **72,** 3186–3190 (2001).

22. T. Sun, Z. Y. Zhang, and K. T. V. Grattan, "Erbium/ytterbium fluorescence based fiber optic temperature sensor system," Rev. Sci. Instrum. **71,** 4017–4022 (2000).

23. Y. N. Ning, A. Meldrum, W. J. Shi, B. T. Meggitt, A. W. Palmer,

K. T. V. Grattan, and L. Li, "Bragg grating sensing instrument using a tuneable Fabry-Perot filter to detect wavelength variations," Meas. Sci. Technol. **9,** 599–606 (1998).

24. Y. M. Gebremichael, B. T. Meggitt, W. J. O. Boyle, W. Li, K. T. V. Grattan, L. Boswell, B. McKinley, K. A. Aarnes, and L. Kvenild, "Multiplexed fibre Bragg grating sensor system for structural integrity monitoring in large civil engineering applications," in *Proceedings of Sensors and their Applications XI*, K. T. V. Grattan and S. H. Khan, eds. (Institute of Physics, London, 2001), pp. 341–345.

25. Z. Y. Zhang, K. T. V. Grattan, Y. Hu, A. W. Palmer, and B. T. Meggitt, "Prony's method for exponential lifetime estimations in fluorescence-based thermometers," Rev. Sci. Instrum. **67,** 2590–2594 (1996).

26. A. Othonos, "Fiber Bragg gratings," in *Optical Fiber Sensor Technology: Advanced Applications*, K. T. V. Grattan and B. T. Meggitt, eds. (Kluwer Academic, Dordrecht, The Netherlands, 2000).

27. Z. Y. Zhang, K. T. V. Grattan, A. W. Palmer, B. T. Meggitt, and T. Sun, "Characterization of erbium-doped intrinsic optical fiber sensor probes at high temperatures," Rev. Sci. Instrum. **69,** 2924–2929 (1998).